

## DATA-DRIVEN APPROACH TO ESTIMATING SOOT DISTRIBUTION INSIDE CATALYTIC FILTERS IN AUTOMOTIVE EXHAUST GAS AFTERTREATMENT

Khýr M. \*, Plachá M. \*\*, Hlavatý T. \*\*\*, Isoz M. †

**Abstract:** *The performance and the necessary regeneration frequency of catalytic filters (CFs) used in the treatment of automotive exhaust gases depend strongly on the solid matter accumulated within their porous walls. Reliable predictions of solid matter (soot) accumulation are crucial in the development and optimisation of CFs. In this contribution, we exploit the tools of artificial intelligence (AI) to estimate the distribution of soot directly in the porous microstructure of CFs. Specifically, our AI model uses deep neural networks (DNNs) and convolutional autoencoders (CAEs) to predict the soot distribution from information about the microstructure and the initial velocity field. To provide the model with training and validation data, we used our previously developed transient numerical model of particle deposition in the CF walls to calculate soot distribution in a dataset of artificial 2D geometries. The results of the developed AI model are in good agreement with simulation regarding the total amount of accumulated soot. However, the accuracy in the spatial distribution of the soot is not optimal, and consequently, using estimated particle deposits to simulate the pressure drop in the artificial microstructure results in 35 % accuracy.*

**Keywords:** AI, DNN, CFD, OpenFOAM, catalytic filters.

### 1. Introduction

The ever-tightening regulation of pollutants in automotive exhaust gas requires more efficient and complex gas aftertreatment systems. Particulate matter in the gas has to be filtered out and pollutant gases have to be converted. These two steps can be combined in one component, the catalytic filter (CF), thus reducing the heat losses and spatial requirements of the aftertreatment process (Kočí et al., 2019). The filtration efficiency and overall pressure drop of the CF are severely affected by the deposition of particulate matter (soot) within its porous walls. Filtration simulations can benefit microstructure design by predicting the distribution of soot.

In our previous work, we studied gas flow and pollutant gas conversion Kočí et al. (2019) and particulate matter filtration (Plachá et al., 2024) at a pore-scale level utilising tools of computational fluid dynamics (CFD). The CFD-based pore-scale numerical solver by Plachá et al. (2024) uses a partially two-way coupled Eulerian-Lagrangian approach to model the transport of solid particles in flowing gas. The solver is capable of predicting the accumulated soot distribution resolved in space and time in good agreement with the experimental data. In this work, we attempt to circumvent the main computational bottleneck of the numerical model, namely the computational cost of particle tracking during the soot deposition modelling. We propose a data-driven approach to estimating the soot distribution, and whilst our ultimate goal is to estimate the spatio-temporal distribution in real-world three-dimensional microstructures, at present we focus solely on soot distribution in two-dimensional artificial geometries at an a priori selected time step.

---

\* Matyáš Khýr: Institute of Thermomechanics, Czech Academy of Sciences (CAS), Dolejškova 1402/5; 182 00, Prague; CZ, khyrm@it.cas.cz

\*\* Ing. Marie Plachá, PhD.: Department of Chemical Engineering, Faculty of Chemical Engineering, University of Chemistry and Technology, Technická 5; 166 28, Prague; CZ

\*\*\* Ing. Tomáš Hlavatý: Institute of Thermomechanics, CAS, Dolejškova 1402/5; 182 00, Prague; CZ

† Ing. Martin Isoz, PhD.: Institute of Thermomechanics, CAS, Dolejškova 1402/5; 182 00, Prague; CZ

In the following text, we will briefly introduce the numerical model by Plachá et al. (2024) and present the developed AI model focussing first on the structural parts; deep neural networks (DNNs) and convolutional autoencoders (CAEs); and then on the complete architecture. Next, we describe the generation of the artificial model dataset and, finally, we show examples of predicted soot distributions and compare the simulated pressure drop between the microstructures with the simulated and estimated soot deposits.

## 2. Mathematical model

**Full-order numerical model.** The training and validation dataset for AI was prepared using the numerical model by Plachá et al. (2024) which was created for simulation of the accumulation of soot within the CF. The model combines two approaches; Eulerian and Lagrangian. The Eulerian approach is used to calculate the flow within the CF microstructure, and the effect of particles on the flow is neglected. The calculated velocity field is then used to simulate the transport of the particulate matter by tracking individual particles via the Lagrangian approach. Interactions between particles are not taken into account, given their small sizes and low concentrations. The two approaches are partially coupled, since the deposited matter is introduced into the computational domain via an algorithm of Isoz and Plachá (2022) where the matter creates a porous zone obstructing the flow and a probabilistic particle trap. Hence, the flow field can be recomputed iteratively and the newly deposited particulate matter is reflected by adjusting the domain.

The SIMPLE algorithm, as implemented in OpenFOAM (OpenCFD, 2007), is used to solve the Navier-Stokes equations in a form describing a steady-state incompressible laminar flow of a Newtonian fluid. The computational domain  $\Omega$  considered here can be divided into three respective sub-domains containing; free pores ( $\Omega_P$ ), catalytic coating ( $\Omega_C$ ), and deposited soot ( $\Omega_S$ ). The governing equations can be written as

$$\begin{aligned} \nabla \cdot (\mathbf{u} \otimes \mathbf{u}) - \nabla \cdot (\nu \nabla \mathbf{u}) &= -\nabla \tilde{p} + \mathbf{s} \\ \nabla \cdot \mathbf{u} &= 0 \end{aligned}, \quad \mathbf{s} = \begin{cases} 0 & \text{in } \Omega_P \\ -\frac{\nu}{\kappa_C} \mathbf{u} & \text{in } \Omega_C \\ -\phi_s \frac{\nu}{\kappa_s} \mathbf{u} & \text{in } \Omega_S \end{cases} \quad (1)$$

where  $\mathbf{u}$  is the gas velocity,  $\nu$  kinematic viscosity and  $\tilde{p}$  the kinematic pressure. The source term  $\mathbf{s}$  is active only in the catalytic coating ( $\Omega_C$ ) and in the deposited soot ( $\Omega_S$ ), as it accounts for additional resistance in these porous regions, calculated based on the Darcy permeability model. Particle tracking implementation reflects Newton's second law of motion

$$m \frac{d^2 \mathbf{r}}{dt^2} = \mathbf{F}_D + \mathbf{F}_B, \quad (2)$$

where  $\mathbf{r}$  is the particle position and  $m$  the particle mass. Two forces acting on the particles are assumed; the drag  $\mathbf{F}_D$  and the Brownian force  $\mathbf{F}_B$ ; other forces are negligible. To calculate the drag, the Stokes law with Cunningham slip correction is used (Plachá et al., 2024). The Brownian force is calculated as in Li and Ahmadi (1993). Furthermore, the model implements the effect of adhesion of the soot via a probabilistic trap. When a particle comes into contact with the walls of the CF or the coating, the probability is set to  $\mathcal{P} = 1$ . In cells with deposited soot, a particle is trapped with probability  $\mathcal{P} = \phi_s$ , where  $\phi_s$  is the volume fraction of soot in the cell. The model is implemented in the OpenFOAM open-source C++ library (OpenCFD, 2007) and its detailed description can be found in Plachá et al. (2024); Isoz and Plachá (2022).

The numerical model was used by Plachá et al. (2024) to perform simulations in 500  $\mu\text{m}$  long segments of the wall of the CF channel, see Fig. 1a. A two-dimensional square cutout with size 80  $\mu\text{m}$  was created as a model geometry for the AI. The cutout captures a single channel the inner dimensions of which were parameterised. Namely, the number of substrate and coating layers on the walls were changed to ensure that the model dataset includes geometries with various structural characteristics, see examples in Fig. 1c.

**Data-driven soot estimation model.** The neural network design stems from our objective to estimate the soot distribution function  $\phi_s^t : \Omega \subset \mathbb{R}^d \rightarrow [0, 1]$ ,  $d = 2, 3$  at an a priori selected time  $t \in (0, T]$  via an approximation of an operator  $\mathcal{G}$ . The operator's arguments are the binary microstructure function  $\mathbf{Z} : \Omega \rightarrow \{0, 1\}^2$  and the initial velocity field  $\mathbf{u} : \Omega \rightarrow \mathbb{R}^d$  in a clean CF. Fundamentally, this approach is inspired by the DeepONet of Shukla et al. (2024). In particular, discrete approximations of  $\mathbf{Z}$  and  $\mathbf{u}$  are processed and a discrete approximation of  $\phi_s^t$  is returned, i.e., we pursue a discrete approximation of  $\mathcal{G}$ .

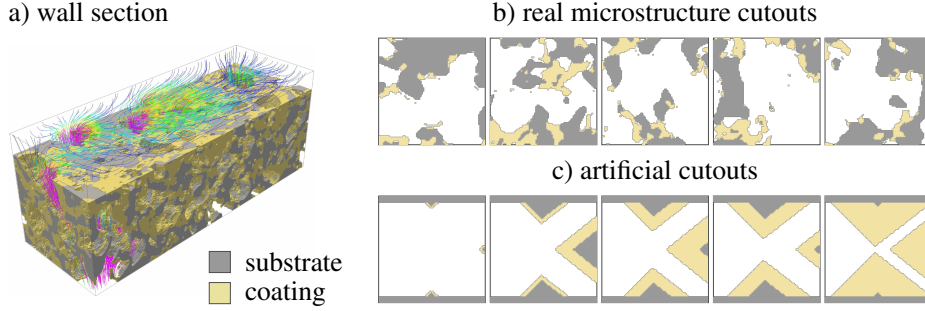


Fig. 1: a) CF wall segment from (Plachá et al., 2020); b) and c) examples of microstructure cutouts.

To efficiently process high-dimensional data, separately trained fully-connected deep neural network and three convolutional autoencoders are used in the model. The microstructure data including substrate ( $\mathbf{Z}_S$ ) and catalytic coating ( $\mathbf{Z}_C$ ) are processed by the first autoencoder, the velocity field ( $\mathbf{u}$ ) by the second and the soot volume fraction field ( $\phi_s^t$ ) by the third. Note that all the fields in the present work are considered to be of dimension  $d = 2$ . Lastly, the field of the volume fraction of soot is estimated by the deep neural network.

Deep neural networks (DNNs) consist of layers of small units, so-called *neurons*. Each neuron represents a function, the function of the  $j$ -th neuron in the  $i$ -th layer can be written as  $o_{ij} = f_{ji}(\mathbf{x})$ . The input of the function ( $\mathbf{x} = \mathbf{o}_{i-1}$ ) is the vector of outputs of neurons forming the  $(i - 1)$ -th layer. The output is a part of inputs to each neuron in the  $(i + 1)$ -th layer. The function  $f_{ij}$  is a composed parametric function  $a_{ij}(\mathbf{w}_{ij}^T \mathbf{o}_{i-1})$ , where  $a$  is the activation function and  $\mathbf{w}$  the weight vector. In matrix-vector notation, the parametric function for  $i$ -th layer can be written as

$$f_i(\mathbf{o}_{i-1}) = \mathbf{a}_i(\mathbf{W}_i^T \mathbf{o}_{i-1}), \quad (3)$$

where  $\mathbf{a}$  is generally non-linear and applied in an element-wise manner on the product of the weight matrix  $\mathbf{W}$  and the previous layer output  $\mathbf{o}_{i-1}$  representing an affine transformation. Training a neural network means adjusting the network weights to minimise the error in fitting the given data.

A convolutional autoencoder is formed of two parts; an encoder and a decoder. The role of the encoder is to gradually reduce the dimensionality of the input data, and it commonly consists of a combination of convolutional and downsampling layers. On the other hand, the decoder uses transposed convolutional layers with strides and/or upsampling to reconstruct high-dimensional data from the low-dimensional representation.

The complete architecture of the AI model comprises two encoders for transforming the high-dimensional input data into low-dimensional latent representations, a DNN for work in the latent space and, a decoder for transformation of the DNN output back. The approximated operator  $\mathcal{G}$  then works in several branches. In the first one, the two matrices  $\mathbf{Z}_S$  and  $\mathbf{Z}_C$  representing the microstructure are given to the pre-trained encoder and they are converted into their latent representation. In the second branch, the flow field data  $\mathbf{u}$  are processed similarly to the first branch. Thereafter, the DNN estimates the latent representation  $\tilde{\phi}_s$  of the desired field  $\phi_s$ . Lastly, the two-dimensional  $\tilde{\phi}_s$  is reconstructed by the pre-trained decoder. The architecture described and data examples are depicted in Fig. 2a.

**Data transfer between full-order model and AI.** The cells of the initial coarse orthogonal computational mesh correspond one-to-one to the elements of the binary matrices  $\mathbf{Z}$ . However, during simulation, the mesh is refined near the edges and in regions with accumulated soot. This leads to a locally refined unstructured mesh from which the results cannot be used directly as input to the encoders. The data from the unstructured mesh must first be mapped back onto a coarse structured orthogonal mesh, and then the cell-centre values can be read and stored in rectangular matrices. Similarly, the estimated values  $\tilde{\phi}_s$  are mapped back onto a coarse mesh and, subsequently, the mesh is refined and used in the simulation to compute the pressure drop.

### 3. Results

Examples of soot distribution estimates compared to simulation together with pressure fields in model geometries calculated with estimated and simulated soot deposits are shown in Fig. 2b. Although the network

was able to capture the general shape of accumulated soot, the mean squared error (MSE) in the estimated soot distributions across the validation dataset is larger than 50 %, since the estimated distributions are more diffuse. This also affects the pressure fields and the calculated pressure drop, which has a mean error 35 % across selected samples.

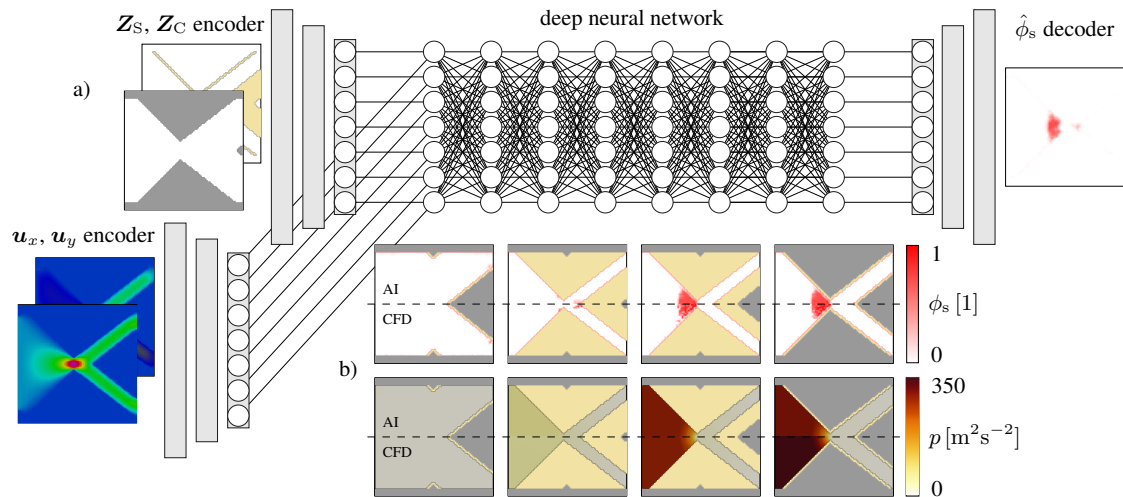


Fig. 2: a) AI model architecture and b) examples of soot distributions and pressure fields in model geometries.

#### 4. Conclusions

We presented the design of a neural network capable of estimating the soot distribution in the catalytic filter walls. We used an existing numerical model to create an artificial model dataset that was then used for network training and validation. We have demonstrated the model's ability to process structural data and provide qualitative estimates of the soot distribution, which are accurate in the total amount of accumulated soot but lack the sharp spatial distribution. Since the smearing present in AI estimates affects the pressure drop, we are currently working to address this before extending the model to three-dimensional geometries.

#### Acknowledgments

The work was financially supported by the institutional support RVO:61388998, by the Czech Science Foundation (GA 22-12227S) and by the grant project with No. TN02000069/001N of the Technology Agency of the Czech Republic.

#### References

- Isoz, M. and Plachá, M. (2022) A parallel algorithm for flux-based bounded scalar redistribution. In *Proceedings of the conference Topical Problems of Fluid Mechanics*. Institute of Thermomechanics of the Czech Academy of Sciences, pp. 87–94.
- Kočí, P., Isoz, M., Plachá, M., Arvajová, A., Václavík, M., Svoboda, M., Price, E., Novák, V., and Thompsett, D. (2019) 3D reconstruction and pore-scale modeling of coated catalytic filters for automotive exhaust gas aftertreatment. *Catalysis Today*, 320, pp. 165–174.
- Li, A. and Ahmadi, G. (1993) Computer simulation of deposition of aerosols in a turbulent channel flow with rough walls. *Aerosol Science and Technology*, 18, pp. 11–24.
- OpenCFD (2007) *OpenFOAM: The Open Source CFD Toolbox. User Guide Version 1.4*, OpenCFD Limited. Reading UK.
- Plachá, M., Isoz, M., Kočí, P., Jones, M., Svoboda, M., Eastwood, D., and York, A. (2024) Particle accumulation model in 3D reconstructed wall of a catalytic filter validated with time-resolved X-ray tomography. *Fuel*, 356, pp. 129603.
- Plachá, M., Kočí, P., Isoz, M., Svoboda, M., Price, E., Thompsett, D., Kallis, K., and Tsolakis, A. (2020) Pore-scale filtration model for coated catalytic filters in automotive exhaust gas aftertreatment. *Chemical Engineering Science*, 226, pp. 115854.
- Shukla, K., Oommen, V., Peyvan, A., Penwarden, M., Plewacki, N., Bravo, L., Ghoshal, A., Kirby, R. M., and Karniadakis, G. E. (2024) Deep neural operators as accurate surrogates for shape optimization. *Engineering Applications of Artificial Intelligence*, 129, pp. 107615.